Structural and Sr^{2+} Ion Exchange Studies of Gallosilicate TsG-1

Yongjae Lee,[†,§] Sun-Jin Kim,[†] Martin A. A. Schoonen,[†] and John B. Parise*[,†,‡]

Departments of Geosciences and Chemistry, State University of New York, Stony Brook, New York 11794-2100

Received December 20, 1999. Revised Manuscript Received March 31, 2000

The potassium gallosilicate TsG-1, $K_{10}Ga_{10}Si_{22}O_{64}\cdot 5H_2O$, when contacted with a Sr^{2+}:Na^+ = 1:5 solution, exhibited a preference for Sr^{2+} as determined from ion-exchange studies using ion chromatography. A structural model for the strontium-exchanged material, Sr-TsG-1, $Sr_5Ga_{10}Si_{22}O_{64}\cdot 19H_2O$, was obtained using Rietveld analysis and high-resolution synchrotron X-ray powder diffraction data. The space group, *Pnma*, of the as-synthesized material is retained in Sr-TsG-1, which has $a = 8.6826(1)$, $b = 13.8828(1)$, $c = 16.2484(1)$ Å. The buckled 8-ring site, consisting of interpenetrated double 6-ring (iD6R) arrays in the CGS topology adopted by TsG-1, is half-occupied by Sr^{2+} to form a distorted tetrahedral coordination with four framework oxygen atoms. The elliptical 8-ring and s-shaped 10-ring, generated by cross-linking the iD6R arrays along the *b* and *a* axis, respectively, also provide environments suitable for Sr^{2+}. An in-situ synchrotron X-ray powder diffraction study confirmed *b* axis contraction upon Sr^{2+} uptake into K-TsG-1. Changes in the ellipticity of the s-shaped 10-ring (Δ10) and elliptical 8-ring (Δ8) were monitored from Rietveld refinements based on these data. An abrupt increase in Δ10 is commensurate with the *b*-axis contraction and suggested a site-specific ion-exchange mechanism. Changes in the cation distribution at each site, however, are not resolved due to a lack of contrast between the effective scattering powers and the interatomic distances involving the sites occupied by Sr^{2+} and K^+ ions.

Introduction

Ion exchange is a useful means to tailor the adsorption and molecular sieving properties of aluminosilicate zeolites,[1,2] and the selective ion-exchange properties of some zeolites make them important in environmental cleanup[3] and industrial applications.[4,5] For example, the mineral clinoptilolite exhibits a preference for alkali and alkaline earth radionuclides such as Cs^+ and Sr^{2+} in the presence of environmentally benign ions such as Na^+ and K^+, making it effective in nuclear wastewater treatment.[3,6]

The ion-exchange properties of zeolites are generally controlled by factors such as the anionic field strength of the aluminosilicate framework and the free energy of hydration of the exchanging cations.[7] Other factors important in determining the ion-exchange selectivity of a given zeolite include structural parameters, such as the framework geometry and connectivity.[7] These affect the sizes of cages and channels as well as the cation coordination environments, which need to be negotiated during the ion-exchange process. Zeolites are also polyfunctional in many cases, containing a variety of exchangeable cation sites, accessible through varying windows and pore geometries.[7] Several studies of aluminosilicate zeolites interpret the observed ion-exchange behavior in terms of the structural parameters of the zeolitic frameworks and are illustrative of site-specific ion-exchange mechanisms.[7−12]

Isomorphous replacement of Si or Al in the aluminosilicate frameworks of zeolites with Ga or Ge is expected to influence ion-exchange properties.[2] Introduction of larger tetrahedral atoms such as Ga or Ge results in modification of the geometries of the molecular-sized cages and channels.[13] Many of the recently synthesized aluminogermanates have Ge/Al ratios of 1.0, maximizing their ion-exchange capacities.[14,15] Further, new framework topologies, unique to gallate or germanate chemistry, can also be generated.[16,17] Investigations on

* To whom correspondence should be addressed. E-mail: John.Parise@sunysb.edu.
† Department of Geosciences.
‡ Department of Chemistry.
§ E-mail: Yongjae.Lee@sunysb.edu.

(1) Breck, D. W. *Zeolite Molecular Sieves*; Krieger: Malabar, FL, 1984.
(2) Barrer, R. M. *Hydrothermal Chemistry of Zeolites*; Academic Press: London, 1982.
(3) Ames, L. L. *Am. Mineral.* **1960**, *45*, 689.
(4) Kuhl, G. H.; Sherry, H. S. Proceedings of the 5th International Conference on Zeolites, 1980, Naples, Italy; p 813.
(5) Borgstedt, E. v. R.; Sherry, H. S.; Slobogin, J. P. *Stud. Surf. Sci. Catal.* **1997**, *105*, 1659.
(6) Pabalan, R. T.; Bertetti, F. P. *Mater. Res. Soc. Symp. Proc.* **1994**, *333*, 731.
(7) Sherry, H. S. In *Ion Exchange. A Series of Advances*; Marinsky, J. A., Ed.; Marcel Dekker: New York, 1969; Vol. 2; p 89.
(8) Sherry, H. S. *J. Phys. Chem.* **1965**, *70*, 1158.
(9) Sherry, H. S. *J. Phys. Chem.* **1968**, *72*, 4086.
(10) Olson, D. H.; Sherry, H. S. *J. Phys. Chem.* **1968**, *72*, 4095.
(11) Lee, Y.; Carr, S. W.; Parise, J. B. *Chem. Mater.* **1998**, *10*, 2561.
(12) Parise, J. B.; Cahill, C. L.; Lee, Y. *Can. Mineral.*, in press.
(13) Meier, W. M.; Olson, D. H.; Baerlocher, C. *Atlas of Zeolite Structure Types*, 4th ed.; Butterworth: London, 1996.
(14) Johnson, G. M.; Lee, Y.; Tripathi, A.; Parise, J. B. *Microporous Mesoporous Mater.* **1999**, *31*, 195.
(15) Johnson, G. M.; Reisner, B. A.; Tripathi, A.; Corbin, D. R.; Toby, B. H.; Parise, J. B. *Chem. Mater.* **1999**, *11*, 2780.
(16) Lee, Y.; Kim, S.-J.; Wu, G.; Parise, J. B. *Chem. Mater.* **1999**, *11*, 879.

10.1021/cm990789g CCC: $19.00
Published on Web 05/23/2000

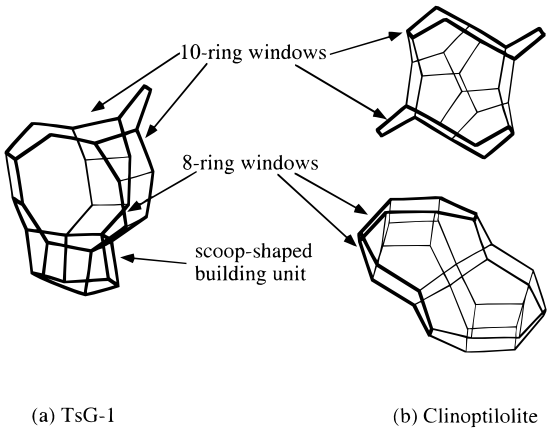

Figure 1. Comparison of the cages found in (a) TsG-1 and (b) clinoptilolite. Nodes represent the T atoms, and straight-line sections represent the T−O−T linkages. Some of the s-shaped 10-rings and elliptical 8-rings are emphasized with bold lines along with the scoop-shaped building unit of TsG-1 (see text).

the ion-exchange properties as a function of framework topology for these new materials can extend our understanding of the ion-exchange process in general.

The structure of the microporous gallosilicate TsG-1,[16,18] $K_{10}Ga_{10}Si_{22}O_{64}\cdot 5H_2O$, possesses the CGS topology.[19] The openings to the cages in TsG-1 are combinations of nonplanar elliptical 8- and 10-rings (Figure 1), similar to those found in clinoptilolite[16,20,21] and suggest that it might exhibit clinoptilolite-like selectivity toward Sr^{2+} and Cs^+ ions.[3,6] Composed of dense layers of the 4−4−1 building unit[1] in the *ac* plane, the cages in clinoptilolite are interconnected in two dimensions (Figure 1b), while those in TsG-1 allow diffusion in three dimensions (Figure 1a). Preliminary results show that Na^+, Rb^+, Cs^+, Sr^{2+}, and NH_4^+ ions can all exchange for K^+ in the as-synthesized material without framework collapse.

As a first step toward understanding of the influence of framework topology, composition, and site geometry on the ion-exchange properties of some Ga/Ge microporous materials, Sr^{2+} exchange into the as-synthesized K-TsG-1 was undertaken. A preliminary study, to determine whether K-TsG-1 is selective toward Sr^{2+} in the presence of Na^+, was performed as a function of time using ion chromatography. Structural responses to Sr^{2+} exchange into K-TsG-1 were monitored as a function of exchange level using a combination of ex-situ and in-situ synchrotron X-ray powder diffraction and Rietveld analysis.

Experimental Section

Starting Material. A powder sample of K-TsG-1 for the measurement of sodium and strontium uptake curves was prepared in a manner similar to that described by Lee et al.[16] An initial characterization of the bulk samples to verify phase identity and purity was performed by powder X-ray diffraction using a Scintag PAD-X automated diffractometer and Cu Kα radiation. A step scan was employed over the 2θ range 3−50° with a step size of 0.02° and a step counting time of 3 s. The single-phase product, which was indexed in an orthorhombic cell with $a = 8.665(1)$, $b = 14.193(1)$, $c = 16.342(1)$ Å, was identified as K-TsG-1. The difference in the *b* axis parameter for the single-crystal study[16] can be related to the different hydration level under which each sample was prepared and the data were collected. The result from the in-situ heating experiment was consistent with this phenomenon and showed that the *b* axis is most sensitive to the changes in hydration level.[16]

Ion Chromatographic Measurements. An aqueous mixture of Sr^{2+}:Na^+ = 1:5 at a total normality of 0.006 N was prepared from reagent-grade $SrCl_2\cdot 6H_2O$ and NaCl. The pH of the unbuffered solution was between 6 and 7. A 0.1 g powder sample of K-TsG-1, equilibrated with water vapor by placing it in a desiccator over a saturated NH_4NO_3 at room temperature for 4 weeks, was added to a 50 mL of the Sr^{2+}/Na^+ aqueous solution. The solid mass to solution volume ratio was chosen to yield considerable differences in cation concentrations in solution as a function of time. The above solid plus solution mixture was contained in a capped polypropylene bottle and stirred at room temperature. Periodically a 0.1 g aliquot was removed from the experiments and diluted with deionized water to a volume of 5 mL. Cation concentrations were determined using a Dionex DX500 ion chromatograph. A CS12 analytical column and a standard methanesulfonic acid eluant were used to separate the cations. A conductivity detector was used to quantify the cation concentration. NIST traceable standards were used to calibrate the instrument. After 7 days of the ion exchange, the solid was separated from the solution by filtering and examined via X-ray powder diffraction. No structural transformations were detected, and the analysis on the peak widths showed that crystallinity remained intact during the exchange process.

Ex-Situ Synchrotron X-ray Powder Diffraction. To examine the structure of Sr^{2+}-exchanged TsG-1 (Sr-TsG-1), ion exchange was performed using 0.1 g of single crystals (150 μm maximum dimension) of K-TsG-1[16] and 500 mL of 0.1 M $SrCl_2\cdot 6H_2O$ solution adjusted to pH 9 with $Sr(OH)_2\cdot 8H_2O$. The solution passed at 0.1 mL/min through a 1.0 mm glass capillary, where the single crystals were held in place with glass fibers at both ends. This procedure was similar to the in-situ ion-exchange setup[12] explained below and chosen to maximize the amount of the solution contacting the crystals without stirring. Three days of ion exchange at room temperature completely removed all residual potassium cations from the crystals, as determined from electron probe micro analysis (EPMA). Attempts to refine the Sr-TsG-1 model using one of the single crystals obtained above, however, failed due to the deterioration of the crystals during the ion-exchange procedure. The ion-exchanged crystals were then ground and equilibrated over saturated NH_4NO_3 for a week prior to the synchrotron X-ray powder diffraction experiment.

Data were collected at beamline X7A of the National Synchrotron Light Source (NSLS). The powdered sample was loaded into a 0.5 mm glass capillary and sealed with an oxygen/methane torch. A channel-cut Ge (111) crystal was used as an incident beam monochromator, and a Ge (220) crystal was placed as a diffracted beam analyzer. The wavelength of 0.7973(1) Å was calibrated using a CeO_2 standard material ($a = 5.4113(1)$ Å). Several low-angle peaks were analyzed, and a step size of 0.004° and a counting time of 5 s over the angular range $4° \le 2\theta \le 47°$ were chosen for data collection. The capillary was rotated at an angular velocity of 1−2 Hz during data collection to obtain better powder averaging.

In-Situ Synchrotron X-ray Powder Diffraction. The pathway of Sr^{2+} exchange into K-TsG-1 was investigated using time-resolved synchrotron powder X-ray diffraction. For this experiment, a translating imaging plate (TIP) detector was coupled to a Small Environmental Cell for Real-Time Studies

(17) Bu, X.; Feng, P.; Stucky, G. D. *J. Am. Chem. Soc.* **1998**, *120*, 11204.
(18) Krutskaya, T. M.; Morozkova, V. E.; Kolishev, A. N. *Izv. Sib. Otd. An. Khim.* **1984**, *5*, 61.
(19) Chippindale, A. M.; Cowley, A. R. *Microporous Mesoporous Mater.* **1998**, *21*, 271.
(20) Stolz, J.; Armbruster, T. Zeolite '97, 5th Int. Conf. on the Occurrence Properties and Utilization of Natural Zeolites, 1997, Ischia, Italy; p 273.
(21) Smyth, J. R.; Spaid, A. T.; Bish, D. L. *Am. Mineral.* **1990**, *75*, 522.

(SECReTS)[22] at the X7B beamline of the NSLS. Single crystals of K-TsG-1[16] were ground and loaded into a 0.7 mm quartz capillary that was plugged with glass fibers at both ends. This capillary was mounted on the SECReTS cell, and a 0.005 M of $SrCl_2 \cdot 6H_2O$ exchange solution passed over the sample using a N_2 overpressure of 20−30 psi at room temperature. The TIP detector recorded the diffraction pattern during the 5 h of the in-situ ion exchange behind a steel slit of width 3 mm with a step size of 0.2 mm and a step counting time of 20 s. The wavelength ($\lambda = 0.9420$ Å), sample to detector distance, zero point, and imaging plate tilt were determined using a LaB_6 standard material prior to the experiment. A more detailed description of the TIP detector geometry and the data processing procedure is found elsewhere.[23,24]

To verify the progress of the in-situ Sr^{2+} exchange into K-TsG-1, two partially Sr^{2+}-exchanged samples were prepared. Two sets of 0.1 g of K-TsG-1 and 500 mL of 0.1 total normality $SrCl_2 \cdot 6H_2O$ and KCl exchange solution were used. The strontium fractions in the initial exchange solutions were 0.3 and 0.9, respectively, and each solution was adjusted to pH 9 with $Sr(OH)_2 \cdot 8H_2O$. After 7 days of exchange at 25 °C, the resultant solids were collected, washed with distilled water, and dried in air. Inductively coupled plasma (ICP) elemental analysis established 35% and 50% Sr^{2+}-exchange levels for the two samples, respectively.

Results and Discussion

Competitive Ion-Exchange Curves for K-TsG-1. Experimental data from the ternary ion exchange are shown in Figure 2. The decrease in both $[Na^+]$ and $[Sr^{2+}]$ in solution is presumed to represent the uptake of these cations into the solid.[25] The increasing $[K^+]$ in solution mirrors the release of this cation from the solid. It is important to note that the strontium concentration in solution continues to decrease even though the molar Na^+/Sr^{2+} ratio increases (Figure 2a). The increase in the sodium concentration in solution between 1 and 5 min of the exchange indicates that the Na^+ ions, loaded during the induction period of the first 1 min, are back-exchanged with Sr^{2+}, the reason for which may be related to the ion selectivity of TsG-1. The release of K^+ from the solid is generally in agreement with the result of the Na^+ and Sr^{2+} uptake although the data are not adjusted for any hydronium exchange which may also have occurred (Figure 2b).

The data in Figure 2 are consistent with TsG-1 exhibiting a preference for Sr^{2+} relative to Na^+ even in a Na^+-rich environment. The characteristic open structure of TsG-1, having the cation sites with the buckled 8- and 10-ring windows, similar to those in clinoptilolite (Figure 1), may provide preferred coordinations for Sr^{2+} as discussed below. More detailed analyses of the ion-exchange kinetics for this and other multicomponent systems[25,26] are planned. For example, these types of experiments have been used to study the mass-transfer mechanisms for chavazite−wastewater interactions.[25] In addition, isotherm studies are underway to determine the selectivity of Sr^{2+} in K-TsG-1.

Ex-Situ Synchrotron X-ray Powder Diffraction. The starting model used for the structure refinement

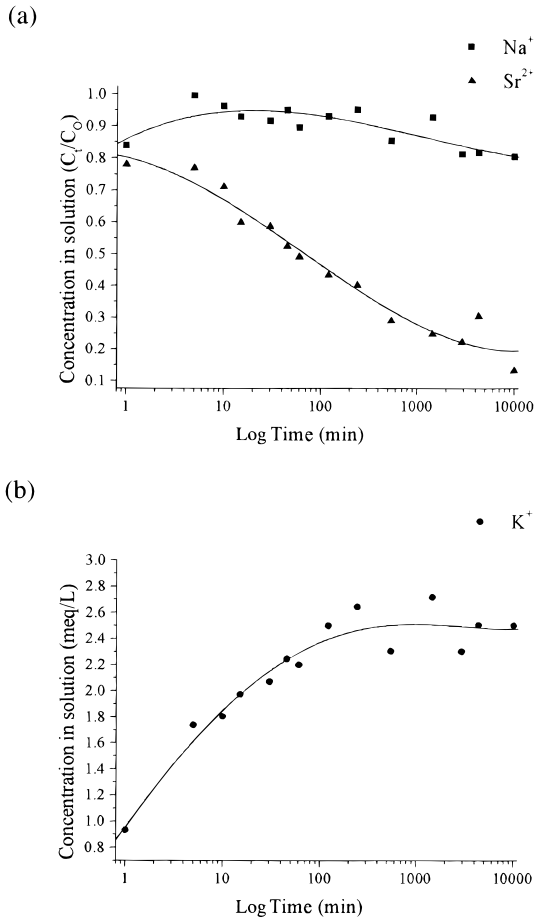

Figure 2. Nonequilibrium ion-exchange curves for (a) Sr^{2+} and Na^+ uptake, and (b) K^+ release. A 0.1 g K-TsG-1 and a 50 mL Sr^{2+}:Na^+ = 1:5 solution at a total normality of 0.006 N were used. C_t and C_o are defined as cation concentrations in solution at time t and 0 min, respectively.

of Sr-TsG-1 was from the single-crystal study of Lee et al.[16] The data were analyzed using the Rietveld Technique[27] in conjunction with the PC-GSAS (General Structure Analysis System) suite of programs.[28] Refinement was performed in the space group *Pnma*. A total of 1098 Bragg reflections were included in the refinement. Interatomic distances derived from the single crystal study were used to supplement the observed data. The T−O distance was set equal to 1.682(1) Å, on the basis of the assumption that the average T−O distance varies linearly with the Ga/Si ratio of 1/2.2.[29] Calculated O−O separation distances of 2.743(5) Å, based on ideal tetrahedral geometry, were also included as soft constraints. The isotropic displacement parameters of the framework T atoms were set equal to one another as were those of the framework oxygen atoms. The isotropic displacement parameters of the nonframework cations and water molecules were fixed according to the result from the single crystal study.[16]

The background was fitted using a 12-term shifted Chebyshev polynomial function. The diffraction peaks were modeled with a pseudo-Voigt function,[30] with

(22) Norby, P.; Cahill, C. L.; Koleda, C.; Parise, J. B. *J. Appl. Crystallogr.* **1998**, *31*, 481.
(23) Norby, P. *J. Appl. Crystallogr.* **1997**, *30*, 21.
(24) Norby, P. *Mater. Sci. Forum* **1996**, *228−231*, 147.
(25) Robinson, S. M.; Arnold, W. D.; Byers, C. H. *AIChE J.* **1994**, *40*, 2045.
(26) Franklin, K. R.; Townsend, R. P. *J. Chem. Soc., Faraday Trans.* **1985**, *81*, 1071.
(27) Rietveld, H. M. *J. Appl. Crystallogr.* **1969**, *2*, 65.
(28) Larson, A. C.; VonDreele, R. B. *GSAS; General Structure Analysis System*; Report LAUR 86-748; Los Alamos National Laboratory: New Mexico, 1986.
(29) Shannon, R. D. *Acta Crystallogr.* **1976**, *A32*, 751.

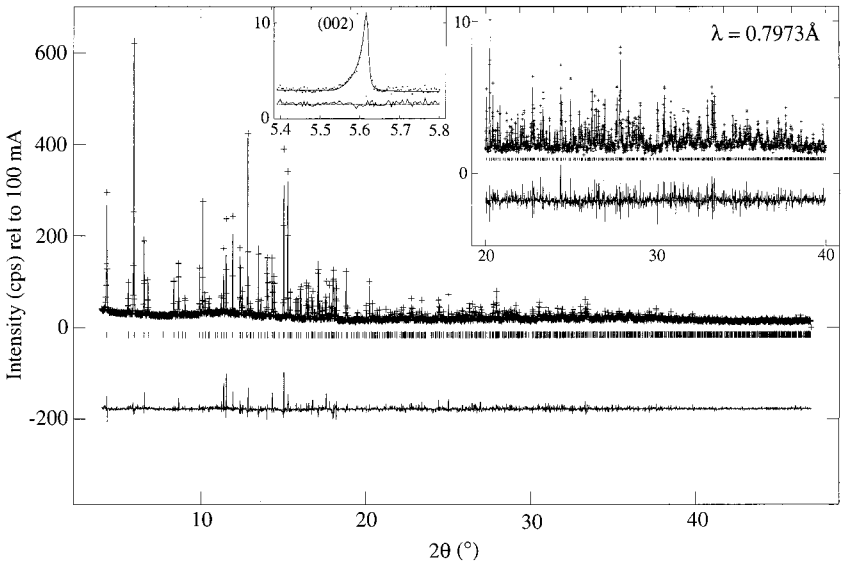

Figure 3. Results of Rietveld refinement of the Sr-TsG-1 model using synchrotron powder X-ray diffraction data at room temperature. A difference curve ($I_{obs} - I_{calc}$) is plotted at the bottom on the same scale. Allowed reflection positions are indicated by vertical lines. The fits in the low- and high-angle portions are emphasized on the top.

calculated asymmetry correction terms[31] introduced in the early stage of the refinement. The extraframework species were located using Fourier difference maps. Three cation sites and five water positions were modeled using scattering factors for Sr and O atoms, respectively, with anomalous scattering terms for Sr of $f' = -2.94$ and $f'' = 0.55$ taken from Cromer's program FPRIME.[32] The occupancies of these sites were refined without any chemical restraints. The final refined number of Sr^{2+} ions is 4.95(8) per unit cell. This is in good agreement with the expected value of 5, which is required for charge compensation of the negatively charged framework, $[Ga_{10}Si_{22}O_{64}]^{10-}$.[16] During the final cycle of the refinement, all positional, fractional and isotropic displacement parameters, profile coefficients, and unit cell and diffractometer zero parameters were varied. The weight of the soft constraints on the framework bond distances was reduced to unity, and the constraints tying the isotropic displacement parameters of the framework species were retained in the final refinement.

The fit of the calculated data for the final refined structural model to the observation is displayed graphically in Figure 3, including details of both an asymmetric low angle peak and high angle data. The residual parameters of the final refinement are $R_{wp} = 12.2\%$, $R_p = 9.2\%$, $R_{F2} = 13.6\%$, and GoF = 2.02. The refined asymmetry parameters of $S/L = 0.0058$ and $H/L = 0.011$ are in good agreement with the initial values of 0.0057 and 0.011, respectively; these values were calculated from the sample to detector distance (L) = 700, detector half size (H) = 8 mm, and the sample half size (S) = 4 mm.[31] Table 1 summarizes the final refined atomic positions and displacement parameters, with selected interatomic distances and angles given in Table 2.

Comparing the unit cell parameters of Sr-TsG-1 (a = 8.6826(1), b = 13.8828(1), c = 16.2484(1) Å) with those of the as-synthesized K-TsG-1 (a = 8.665(1), b = 14.193(1), c = 16.342(1) Å), we find that changes are greatest for the b-axis contraction upon Sr^{2+} exchange. This is analogous with the previous observation where different hydration conditions between single crystal and powder samples of K-TsG-1 caused a considerable difference in the b-axis parameter.[16] The average ⟨T−O−T⟩ bond angle of Sr-TsG-1 is slightly larger than that of K-TsG-1 (Table 2).[16] Specifically, the relatively large increase in the T−O4−T bond angle from 140.1(3)° to 143.4(5)° is related to the changes of the s-shaped 10-ring geometry and, consequently, to the decrease in the b-axis parameter. This is discussed in detail in the in-situ section below.

The buckled 8-ring site of the iD6R, labeled as Sr1 in Figures 1 and 4a, is half-filled with Sr^{2+} ions (Table 1). Four framework oxygen atoms coordinate to the strontium at this site to form a distorted tetrahedron. The

Table 1. Atomic Coordinates and Esd's of Sr-TsG-1[a]

atom	site	p	x	y	z	U_{iso}[b]
T1[c]	8d	1.000	0.5958(2)	0.0405(2)	0.6290(2)	0.014(1)[d]
T2[c]	8d	1.000	0.1793(2)	−0.1345(2)	0.6596(2)	0.014(1)[d]
T3[c]	8d	1.000	0.8861(2)	−0.0173(2)	0.7175(2)	0.014(1)[d]
T4[c]	8d	1.000	0.4521(2)	−0.1384(2)	0.5378(2)	0.014(1)[d]
O1	8d	1.000	0.5843(8)	−0.0671(4)	0.5828(6)	0.031(2)[e]
O2	8d	1.000	0.7774(6)	0.0578(5)	0.6612(6)	0.031(2)[e]
O3	8d	1.000	0.5423(12)	0.1302(5)	0.5654(3)	0.031(2)[e]
O4	8d	1.000	0.9718(10)	0.0475(5)	0.7916(4)	0.031(2)[e]
O5	8d	1.000	0.2808(11)	−0.1087(5)	0.7449(4)	0.031(2)[e]
O6	4c	1.000	0.1237(12)	−0.2500(0)	0.6654(8)	0.031(2)[e]
O7	8d	1.000	0.2743(6)	−0.1121(7)	0.5717(4)	0.031(2)[e]
O8	8d	1.000	0.0223(7)	−0.0634(6)	0.6552(4)	0.031(2)[e]
O9	4c	1.000	0.4998(14)	−0.2500(0)	0.5675(7)	0.031(2)[e]
Sr1	4c	0.488(3)	0.796(1)	−0.250(0)	0.631(1)	0.038[f]
Sr2	8d	0.174(3)	0.067(1)	0.045(1)	0.500(1)	0.038[f]
Sr3	4c	0.40(1)	0.397(1)	0.250(0)	0.664(1)	0.038[f]
OW1	4c	0.83(2)	0.953(3)	0.250(0)	0.538(2)	0.09[g]
OW2	4c	0.47(5)	0.806(1)	0.250(0)	0.874(5)	0.09[g]
OW3	4c	0.90(2)	0.821(3)	0.250(0)	0.673(2)	0.09[g]
OW4	4c	0.86(2)	0.607(3)	0.250(0)	0.765(2)	0.09[g]
OW5	8d	0.88(2)	0.175(2)	0.140(1)	0.568(1)	0.09[g]

[a] Estimated standard deviations are in parentheses. [b] U_{iso} (Å^2). [c] Gallium occupancy of 0.308(3). [d,e] Isotropic displacement parameters constrained to be equal. [f,g] Isotropic displacement parameters fixed.

(30) Thompson, P.; Cox, D. E.; Hastings, J. B. *J. Appl. Crystallogr.* **1987**, *20*, 79.
(31) Finger, L. W.; Cox, D. E.; Jephcoat, A. P. *J. Appl. Crystallogr.* **1994**, *27*, 892.
(32) Cromer, D. T. *J. Appl. Crystallogr.* **1983**, *16*, 437.

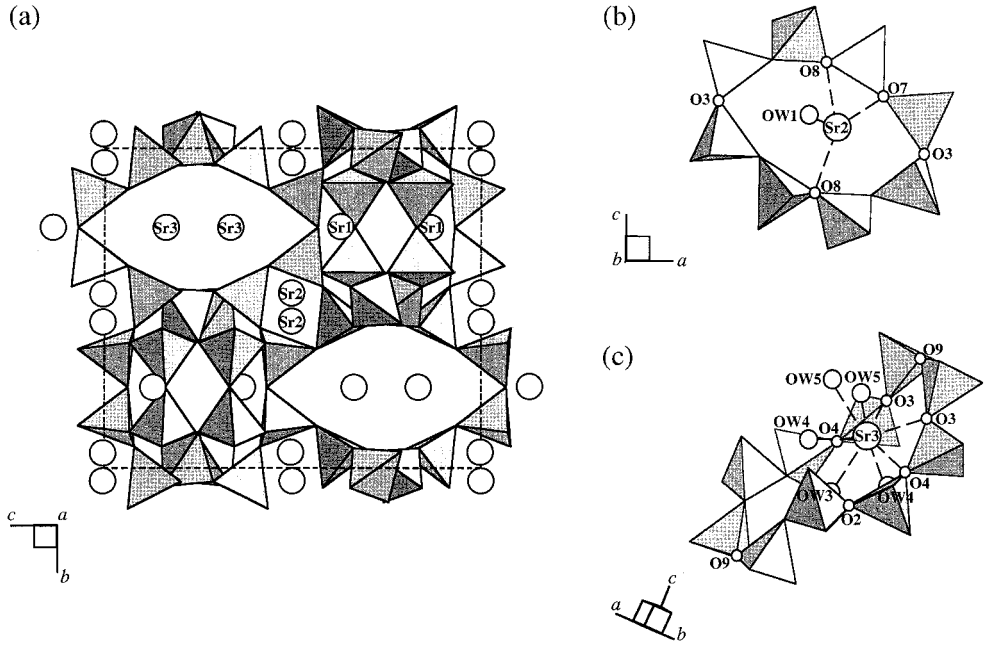

Figure 4. (a) A polyhedral representation viewed down approximately [100] of the Sr-TsG-1 showing the distribution of the strontium cations (open circles) (water molecules are omitted for clarity), (b) strontium cation coordination of the elliptical 8-ring window perpendicular to [010], and (c) strontium cation coordination of the s-shaped 10-ring window.

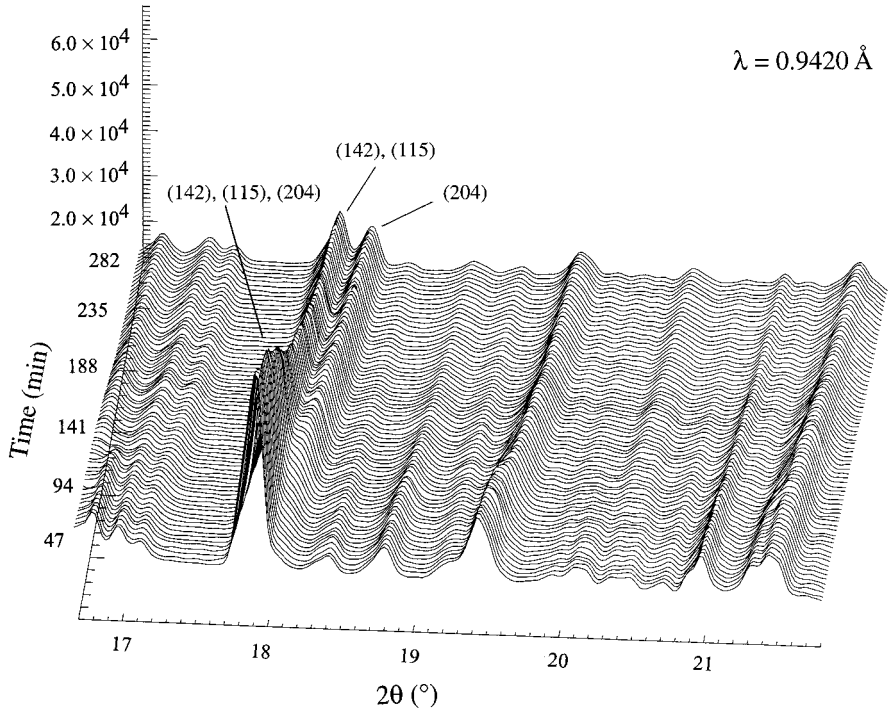

Figure 5. Plot of the synchrotron X-ray powder diffraction profiles as a function of time during the 5 h of Sr^{2+} exchange into K-TsG-1. The patterns are obtained by integrating the imaging plate vertically with an integration width of 3 mm, about the size of the slit.

Sr1−O distances are in the range of 2.77(1)−2.90(1) Å (Table 2). No water molecules are found near the Sr1 site. The Sr2 site in the elliptical 8-ring is partially populated by Sr^{2+} ions (Figure 4b and Table 1). The proximity of this site, separated from each other by 1.70(3) Å across the *a*-glide plane, limits the maximum theoretical occupancy to be less than 0.5 (Table 1). Three framework oxygen atoms and one water molecule (OW1) coordinate to the strontium at the Sr2 site with interatomic distances in the range from 2.65(2) to 3.08(2) Å (Table 2). The s-shaped 10-ring also provides a coordination environment for Sr^{2+} ions at the Sr3 site (Figures 1 and 4c). This site is located on the mirror plane perpendicular to the *b* axis, and the strontium cations are 9-fold coordinated by four framework oxygen atoms and five water molecules (Tables 1 and 2). Interatomic distances of Sr3−O are in the range from 2.45(3) to 2.97(1) Å (Table 2). In comparison, strontium cations occupying the 10-ring site of the Sr^{2+}-exchanged heulandite, a low-silica variant of clinoptilolite, are 7-fold coordinated by two framework oxygen atoms and five water molecules.[20]

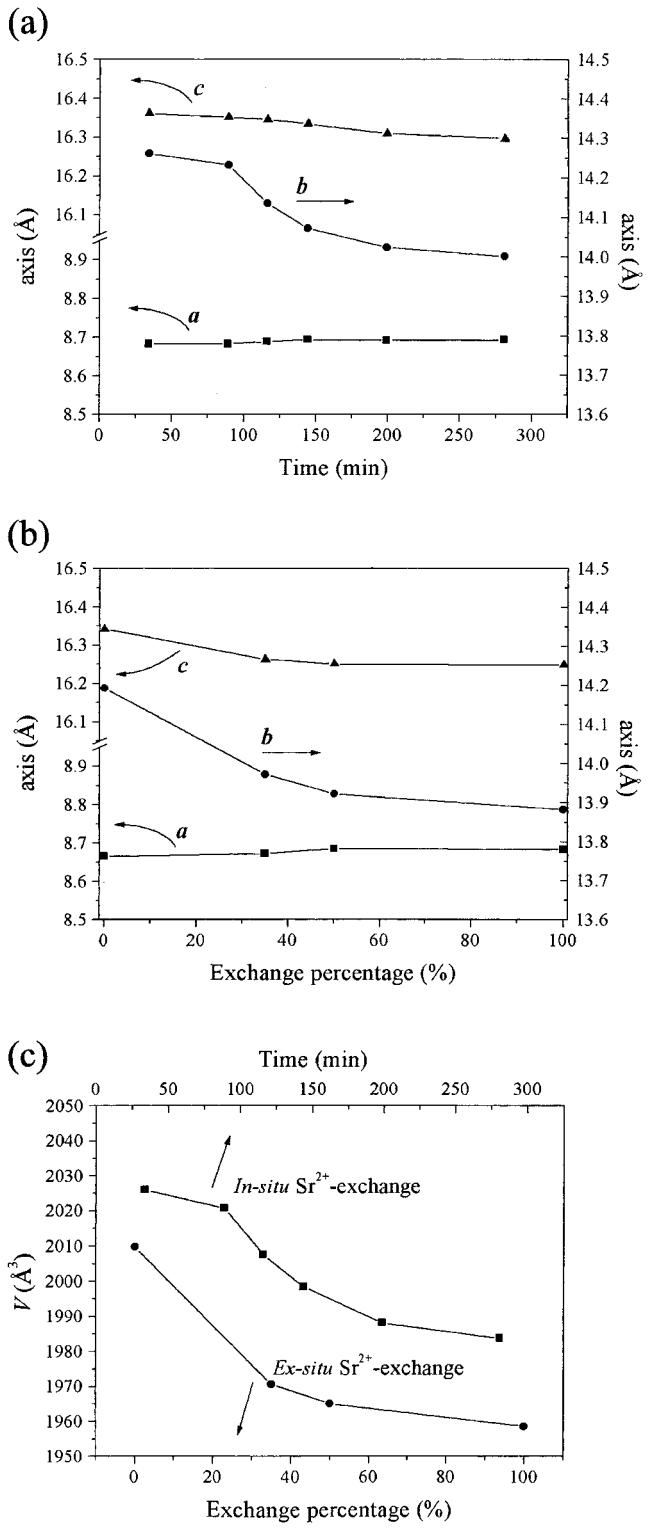

Figure 6. Variations of the unit cell parameters during the (a) in-situ and (b) ex-situ Sr^{2+} exchange into K-TsG-1; and (c) variations of the unit cell volume in both measurements (hydration levels are different between the two experimental conditions, see text).

Water molecules are distributed at five different positions with interatomic distances to Sr^{2+} ions in the range of 2.45(3)−3.08(2) Å (Tables 1 and 2). In particular, the OW2 and OW3 sites exhibit close separation distances to framework oxygen atoms, 2.82(5) and 2.70(1) Å, respectively (Table 2). This was not observed in the K-TsG-1 model, which might be related to the fact that the total number of cations in Sr-TsG-1 is half of that in K-TsG-1, implying more spaces for absorbed water molecules. The refined number of water molecules is 19.3(6) per unit cell in Sr-TsG-1, compared to 4.9(6) in K-TsG-1 (Table 1).[16]

Table 2. Selected Interatomic Distances (Å) and Angles (deg) of Sr-TsG-1[a]

T1−O1	1.674(3)	T3−O2	1.678(3)
T1−O2	1.679(3)	T3−O4	1.677(3)
T1−O3	1.685(3)	T3−O5	1.678(3)
T1−O4	1.682(3)	T3−O8	1.684(3)
av. T1−O	1.680(2)[b]	av. T3−O	1.679(2)[b]
T2−O5	1.682(3)	T4−O1	1.683(3)
T2−O6	1.677(3)	T4−O3	1.681(3)
T2−O7	1.678(3)	T4−O7	1.679(3)
T2−O8	1.684(3)	T4−O9	1.675(3)
av. T2−O	1.680(2)[b]	av. T4−O	1.680(2)[b]
av. O−T1−O	109.5(2)[b]	av. O−T3−O	109.4(2)[b]
av. O−T2−O	109.5(2)[b]	av. O−T4−O	109.4(2)[b]
T1−O1−T4	139.5(5)	T2−O6−T2	145.9(7)
T1−O2−T3	127.5(4)	T2−O7−T4	133.7(3)
T1−O3−T4	130.8(4)	T2−O8−T3	139.9(4)
T1−O4−T3	143.4(5)	T4−O9−T4	135.4(6)
T2−O5−T3	138.3(5)	Av. T−O−T	137.2(2)[b]
Sr1−O9	2.77(1)	OW2−O3	2.82(5) × 2
Sr1−O5	2.81(1) × 2	OW2−OW4	2.47(6)
Sr1−O6	2.90(1)	OW3−O2	2.70(1) × 2
Sr2−O8	2.65(2)	OW3−Sr3	2.73(3)
Sr2−O7	3.06(2)	OW3−OW4	2.69(3)
Sr2−O8	2.96(2)	OW4−Sr3	2.45(3)
Sr3−O3	2.63(1) × 2	OW4−Sr3	2.77(3)
Sr3−O4	2.97(1) × 2	OW4−OW5	3.18(3) × 2
OW1−Sr2	3.08(2)	OW5−Sr3	2.92(2) × 2
OW1−OW5	2.51(2)	OW5−OW5	3.07(4)

[a] Estimated standard deviations are in parentheses. [b] Standard deviations computed using $\sigma = 1/n[\sum_{i=1}^{n}\sigma_i^2]^{1/2}$.

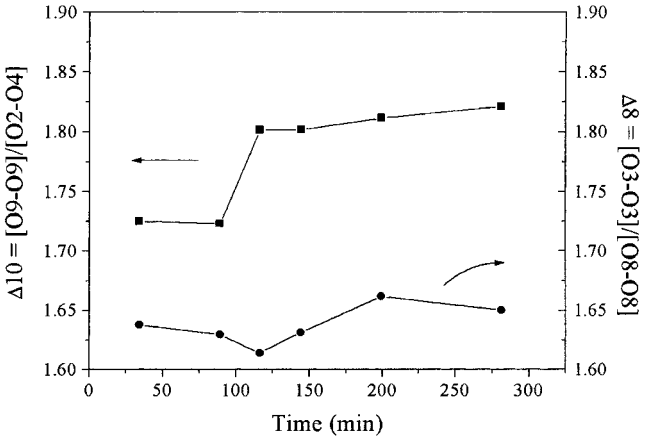

Figure 7. Variations of the ellipticity of the s-shaped 10-ring (Δ10) and elliptical 8-ring (Δ8) during the in-situ Sr^{2+} exchange into K-TsG-1 (also see Figure 4).

In-Situ Synchrotron X-ray Powder Diffraction. Time-resolved synchrotron X-ray powder diffraction spectra obtained during the 5 h of the in-situ Sr^{2+} exchange into K-TsG-1 are shown in Figure 5. One set of peaks, which could be indexed on a primitive orthorhombic cell, was observed throughout the in-situ scan. Changes in the lattice parameters and unit cell volume were analyzed using sets of data integrated to represent 10 min portions during the in-situ scan (Figure 6). A decrease in the *b* axis from 14.271(1) to 14.002(1) Å marked the most change during the in-situ Sr^{2+} exchange. Only a small decrease and increase in the *c* and *a* axes, respectively, accompanied the contraction of the

b axis. The lattice parameters of the two end-members of the Sr-K-TsG-1 as well as 35% and 50% Sr^{2+}-exchanged TsG-1 from the ex-situ study are also plotted for comparison in Figure 6. The lattice parameters determined from the in-situ study are consistently larger than those from the ex-situ study because of the different level of hydration (see Experimental Section).

Rietveld analysis[27] was performed with the sets of data extracted from the in-situ scan. The changes in the ellipticity of the s-shaped 10-ring and elliptical 8-ring, defined as $\Delta 10 = [O9-O9]/[O2-O4]$ and $\Delta 8 = [O3-O3]/[O8-O8]$, respectively (parts b and c of Figure 4), are shown in Figure 7. The abrupt increase of $\Delta 10$ is related to the contraction of the *b* axis, while $\Delta 8$ shows no particular trend during the course of the in-situ Sr^{2+} exchange. Changes in cation distribution may be related to the observed framework responses. Previous studies showed that some selectivity reversals, or anomalous isotherm behaviors upon ion exchange, are caused by site-specific cation distribution at each exchange level. For example, the structural analyses for both $Sr^{2+}-Na^+$ exchange into zeolite X[10] and K^+-Na^+ exchange into zeolite LSX,[11] indicated that abrupt changes in cell parameters correspond to site-specific ion exchange in these materials. Unfortunately, the effective scattering powers of $Sr^{2+}/2$ and K^+ are about the same; they populate similar sites in the occupancy ratio of about 1:2 in TsG-1. This fact, coupled with the similar ionic radii of Sr^{2+} and K^+ based on bond distances (Table 2),[16] hampered discrimination of these cations.

Conclusion

The strontium ion exchange into the potassium gallosilicate TsG-1 was performed via a combination of ion uptake curves and ex-situ and in-situ synchrotron X-ray powder diffraction. During the competitive ion exchange using a 0.1 g K-TsG-1 and a 50 mL $Sr^{2+}:Na^+ = 1:5$ solution at a total normality of 0.006 N, the strontium concentration in solution continued to decrease even though that the molar Na^+/Sr^{2+} ratio increased, indicating a preference of TsG-1 for the strontium. The cation distribution of Sr^{2+}-exchanged TsG-1 is akin to that of the as-synthesized K-TsG-1; Sr^{2+} ions replace K^+ at the nonplanar elliptical 8- and 10-ring sites in about $K^+/Sr^{2+} = 2/1$ ratio. The *b*-axis contraction upon Sr^{2+} exchange is commensurate with the changes in the ellipticity of the s-shaped 10-ring openings, which is suggestive of a site-specific ion-exchange mechanism. To discern cation and site selectivities, isotherm studies and structural investigations of Na^+, Rb^+, Cs^+, and Sr^{2+} exchange into TsG-1 are ongoing.

Acknowledgment. The authors thank the NSF (Grant DMR 97-13375) for financial support. Research carried out in part at the NSLS at Brookhaven National Laboratory is supported by the U.S. Department of Energy, Division of Materials Sciences and Division of Chemical Sciences (grant DE-AC02-98CH10886 for the X7A beamline and grant DE-AC02-98CH10886 for the X7B beamline). Special thanks to Dave E. Cox of beamline X7A and Jonathan C. Hanson of beamline X7B of the NSLS for their help with data collection. Y. Lee also thanks Thomas Armbruster and Barbara Reisner for valuable suggestions, and S.-J. Kim is grateful for the partial support from Korea Institute of Science and Technology (KIST) and Korea Science and Engineering Foundation (KOSEF).

CM990789G